Journal of Power Sources 278 (2015) 197–202

Contents lists available at ScienceDirect

Journal of Power Sources

journal homepage: www.elsevier.com/locate/jpowsour

Short communication

Insertion energetics of lithium, sodium, and magnesium in crystalline and amorphous titanium dioxide: A comparative first-principles study

Fleur Legrain, Oleksandr Malyi, Sergei Manzhos*

Department of Mechanical Engineering, National University of Singapore, Block EA #07-08, 9 Engineering Drive 1, Singapore 117576, Singapore

HIGHLIGHTS

- Insertion of Li, Na, Mg into TiO_2 studied ab initio.
- Compared anatase, rutile, (B), and amorphous TiO_2.
- (B)–TiO_2 binds Li, Na, Mg the strongest among crystalline phases.
- Amorphous TiO_2 binds Li, Na, Mg strongest of all.
- Correct electronic structure with GGA.

ARTICLE INFO

Article history:
Received 8 October 2014
Received in revised form
14 November 2014
Accepted 14 December 2014
Available online 17 December 2014

Keywords:
Titanium dioxide
Amorphous
Lithium ion batteries
Sodium ion batteries
Magnesium ion batteries

ABSTRACT

Titanium dioxide (TiO_2) has been proposed as a potential electrode material for lithium, sodium, and magnesium ion batteries. Among the phases of TiO_2, anatase, rutile, and (B)–TiO_2 are the most commonly used phases for electrochemical storage, while the amorphous phase has also been shown to be a promising candidate. We present a comparative density functional theory study of the insertion energetics of Li, Na, and Mg into anatase, rutile, and (B)–TiO_2, as well as into the amorphous phase. Our results show that among the crystalline phases, (B)–TiO_2 provides the strongest binding between TiO_2 and the inserted Li/Na/Mg atom. We also find that for all Li, Na, and Mg, the amorphous phase provides insertion sites well-dispersed in energies, with a lowest energy site more thermodynamically favorable than insertion sites in the crystalline phases. We also obtain the localized Ti^{3+} states together with the formation of the defect states in the band gap, which are induced by the insertion, at the GGA level of theory (without the Hubbard correction).

1. Introduction

Being abundant, cheap, and safe, titanium dioxide (TiO_2) is widely used in diverse applications, such as catalysis [1,2] and energy conversion [3–6]. It has also emerged as a promising material for Li, Na, and Mg electrochemical storage [7–12]. Its high stability with most organic electrolytes [13] can prevent the formation of the SEI (solid electrolyte interphase), and therefore provides a very high cycle life as well as the possibility to charge/discharge the material at a very high rate [14,15]. For applications in electrochemical storage, the interaction energy of metal atoms such as Li, Na, and Mg with the host structure is a critical parameter determining the suitability of the material as an electrode material as well as its voltage [16,17]. While batteries operate by insertion-deinsertion of small to large amounts of metal up to the theoretical capacity, insertion of small amounts of metal is also important for dye-sensitized solar cells, where Li, Na, and Mg salts are used in the electrolyte to control the energy of the conduction band minimum [18–22].

Li, Na, and Mg intercalation into TiO_2 has been studied theoretically and experimentally but never for all Li, Na, and Mg and all anatase, rutile, and (B)–TiO_2 with the same experimental/computational parameters. A truly comparative study is therefore as of now non-existent. For Li, the three most common phases for electrochemical storage, which are anatase, rutile, and (B)–TiO_2, are known to work well [7,12]. For Mg, experiments have been carried out for rutile [10] and anatase [23], showing that Mg intercalates in these two phases. For Na, (B)–TiO_2 has been shown to work [9], while no electrochemical activity has been observed in rutile [24].

* Corresponding author.
E-mail address: mpemanzh@nus.edu.sg (S. Manzhos).

http://dx.doi.org/10.1016/j.jpowsour.2014.12.058
0378-7753/

In anatase, however, Na intercalation appears to be subject to contradictory (experimental) evidence [8,24]; sodiation-induced phase transformation of anatase has been observed [6]. The difference between the experimental results reported for Na in anatase can be due to many factors (e.g. impurities, nanosizing effects). Computational studies can help rationalize the insertion process and establish theoretical limits on voltages, rates, capacities etc. of various phases and for the insertion of different types of alkali atoms. This is important to guide experimental optimization of electrodes. Yet, very few computational studies are available for Na and Mg intercalation in these crystalline phases of TiO_2 [25]. Moreover, the use of amorphous TiO_2 (*a*-TiO_2) is very little explored both experimentally and theoretically; this is also true for Li insertion, for which the crystalline phases have been extensively studied [26–34]. However, the few studies that did explore *a*-TiO_2 suggest that it can be a promising material, especially for electrochemical storage [24,35–39], although applications in photocatalysis and solar energy conversion are also eyed [40–42].

While several computational studies reported Li insertion energetics into various crystalline phases [28–34], there is, to the best of our knowledge, no ab initio study comparing with the same computational setup the insertion energetics into anatase, rutile, (B)–TiO_2 and amorphous TiO_2 of Li, Na, and Mg. In this paper, we attempt to fill this knowledge gap, and more importantly, we investigate the potential of *a*-TiO_2 as a potential electrode material for all Li-, Na-, and Mg-ion batteries.

2. Methods

Structures were optimized using DFT (density functional theory) [43] and the PBE functional [44]. Core electrons were replaced with Troullier-Martins pseudopotentials [45]. Calculations were done using the SIESTA code [46]. A DZP (double-ζ polarized) basis was generated by SIESTA with the parameters PAO EnergyShift of 0.001 Ry for Ti and O, 0.008 Ry for Na and Mg, and 0.02 Ry for Li. The basis set reproduces the cohesive energy of Li (computed at −1.67 eV vs. the reference value of −1.66 eV [47]), Na (−1.14 eV vs. −1.13 eV [47]) and Mg (−1.55 vs. −1.54 eV [47]), where the experimental values are adjusted for the effect of zero-point motion, with zero-point energy (ZPE) corrections computed to be 0.034 eV, 0.016 eV and 0.029 eV, respectively. The cohesive energies of TiO_2 were computed at −21.29 eV and −21.31 eV for anatase and rutile, respectively, vs. the reference value of −19.9 eV for rutile [48] and in agreement with the fact that the cohesive energy of anatase is 0.012–0.015 eV weaker than that of rutile [49,50]. The numbers are also in agreement with the range of the other reported DFT (PBE) values form −18.77 to −21.44 eV [51,52] and from −21.54 to −21.60 eV [52,53] for rutile and anatase, respectively. Structures were optimized until forces on all atoms were below 0.03 eV/Å and 0.04 eV/Å for crystalline and amorphous structures, respectively. It should be noted that the lowest energy configurations in amorphous TiO_2 were also optimized at a higher accuracy (0.02 eV/Å) but the largest deviation in defect formation energies was found to be less than 0.01 eV. Spin-polarized calculations were performed.

For *a*-TiO_2, a 192-atom supercell of size about 13 × 13 × 13 $Å^3$ was used. The initial structure was taken from Ref. [54] and re-optimized with the present setup. The structure was shown to provide a range of Ti coordination numbers in agreement with experiment, see Ref. [54] for details. The structure was preserved upon relaxation with the present setup, with minor atomic relaxations. The average coordination number of Ti (with a cutoff for the Ti–O bond of 2.5 Å) is 5.7 in our relaxed structure, in good agreement with the measured value of 5.6 [55], vs. 6 in the crystalline titania. Due to the large cell size, the Brillouin zone was sampled at the Γ point, and the TiO_2 cell was first relaxed (until the stresses were below 0.1 GPa) and then held at fixed size during Li, Na, and Mg insertion. The energy cutoff for the Fourier expansion of the density was set to 100 Ry.

For the crystalline phases, a 3 × 3 × 1 cell was used for anatase (~11 × 11 × 10 $Å^3$), 2 × 2 × 4 for rutile (~9 × 9 × 12 $Å^3$), and 1 × 3 × 2 for bronze (~12 × 11 × 13 $Å^3$). The lattice vectors were allowed to relax upon metal insertion. The Brillouin zone was sampled with a 3 × 3 × 3 Monkhorst-Pack point grid, and a 200 Ry cutoff was used for the expansion of the density. We note that different energy cutoffs (for the Fourier expansion of the density) and k-meshes were needed for the convergence of the defect formation energies in amorphous and crystalline TiO_2. Yet, because the defect formation energies are converged, this doesn't undermine the comparison between the different systems. In the amorphous phase, the energy differences for the lowest energy insertion sites (Li, Na, and Mg) were about 0.01 eV when using 2 × 2 × 2 *k* points and within 0.04 eV when increasing the density cutoff to 200 Ry, while in the crystalline phases, the energy differences between 2 × 2 × 2 and 3 × 3 × 3 *k* points were within 0.005 eV and those between 200 and 300 Ry were within 0.02 eV, except for Na in rutile, at 0.035 eV. This convergence allowed us to search for the most favorable insertion sites (in the crystalline phases) with smaller cutoffs and k-grids, while the final insertion energetics were computed from calculations run with the tighter convergence criteria described above.

To identify possible insertion sites in *a*-TiO_2, we covered the simulation cell with a uniform grid of points spaced by 0.2 Å. We then performed a K-means clustering analysis [56,57] on points located farther than 1.5 Å from Ti and O atoms. The algorithm was made identify an increasing number of clusters. Up to 32 clusters were identified with the distance between the centers of the clusters larger than 2.5 Å. Those were used as initial guesses of insertion sites (see Fig. 1), further optimized by DFT. To identify possible insertion sites in crystalline TiO_2 structures, previously reported insertion sites were used [27,31,34]. In total, 117 insertion sites/energies were analyzed across the four phases and three types of inserted atoms.

At the insertion sites, the defect formation energy E_f was computed as:

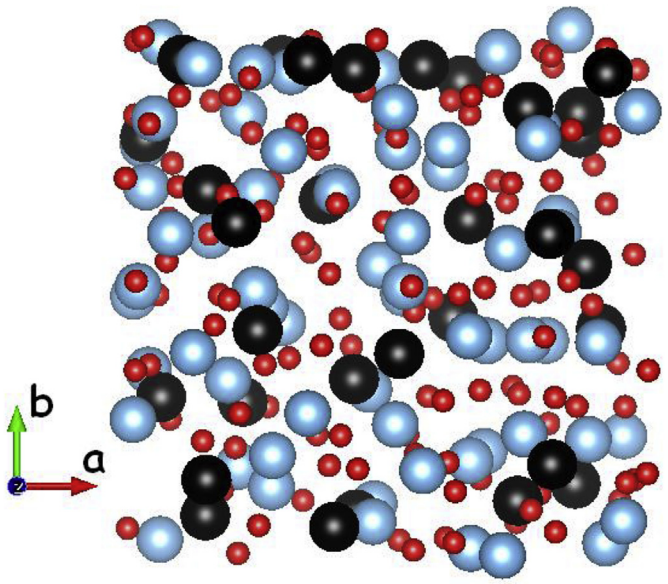

Fig. 1. Atomic structure of the amorphous TiO_2 supercell (Ti – blue atoms, O – red atoms) and locations of the 32 sites identified with K-means clustering analysis (black atoms). (For interpretation of the references to colour in this figure legend, the reader is referred to the web version of this article.)